Available online at www.sciencedirect.com
SCIENCE DIRECT®
International Journal of Mass Spectrometry 233 (2004) 75–80
International Journal of Mass Spectrometry
www.elsevier.com/locate/ijms

Angular momentum coupling and electron-impact excitation cross sections of rare-gas atoms

Tobin Weber, John B. Boffard, Chun C. Lin*

Department of Physics, University of Wisconsin, Madison, WI 53706, USA

Received 3 October 2003; accepted 11 November 2003

Abstract

Electron-impact excitation cross sections for the heavy rare gases are examined in the context of the angular momentum coupling of the final states. Measurements for excitation into $n'p^5np$ levels with $J = 0$ are found to vary in a common way for excitation of Ne, Ar, Kr, and Xe.

Keywords: Electron impact; Excitation cross section; Argon; Neon; Krypton

1. Introduction

Electron-impact excitation of rare gases has been a subject of interest for decades. The large number of excited states and the complexity of their electronic structures make comprehensive studies toward understanding the basic physics an especially challenging task. In addition to their intrinsic fundamental interest, electron-impact excitation and ionization of atoms play a central role in the understanding of many plasmas and discharges such as fluorescent lighting, plasma displays, semiconductor processing, gas-discharge lasers, and atmospheric phenomena. For rare-gases an excited electron configuration may contain numerous levels and the cross sections for excitation into individual levels within the same configuration can vary dramatically in magnitude and energy dependence. For instance, if one is interested in the emission of a neon discharge, it is important to understand the variation in cross sections among the individual levels [1].

For orientation let us consider the $1s^2 2s^2 2p^5 3p$ configuration ($2p^5 3p$) of Ne. The $2p^5$ core has orbital angular momentum l_c and a spin angular momentum s_c equal to 1 and 1/2, respectively. Likewise the 3p "outer" electron is characterized by the corresponding quantities $l_o = 1$ and $s_o = 1/2$. Addition of $\vec{l}_c$, $\vec{s}_c$, $\vec{l}_o$, and $\vec{s}_o$ to form the total angular momentum $\vec{J}$ gives rise to 10 levels with J values ranging from 0 to 3. The coupling of the various angular momentum vectors does not conform to any of the standard coupling schemes such as *LS*, *jj*, and *jK*. The relation between this intermediate coupling and the *electronic structure* of the excited states has been treated extensively in the literature. In this paper we discuss how the *electron-impact cross sections* of the individual levels are affected by the angular momentum coupling. Consideration of the vector coupling allows us to understand the gross features of the cross sections from a physical standpoint without resorting to elaborate calculations.

2. Measurement of optical emission cross sections

In this work we measure the electron-impact excitation cross section *into* a level by detecting the optical emissions *out* of the level [2]. A mono-energetic electron beam is passed through a chamber that has initially been evacuated to 10^{-8} Torr and then back filled to a pressure of 1–10 mTorr with research grade gas. The total electron beam current (I) is measured with a deep Faraday cup which has a narrow slit cut in the side to allow the detection of emissions from the decay of excited atoms. Photons from a particular $i \rightarrow j$ transition are selected using a 1.26 m monochromator and detected using a photomultiplier tube (PMT). The PMT signal is converted to an absolute photon flux (per unit beam

* Corresponding author. Tel.: +1-608-262-0697.
E-mail address: cclin@facstaff.wisc.edu (C.C. Lin).

1387-3806/$ – see front matter © 2004 Elsevier B.V. All rights reserved.
doi:10.1016/j.ijms.2003.11.015

length), Φ, using the known solid angle of the optical system while the wavelength dependent efficiency of the PMT and monochromator is found by measuring the signal from a spectral irradiance standard lamp. In terms of these experimentally measured quantities, the optical emission cross section at an incident electron energy E for the $i \rightarrow j$ transition is defined to be:

$$Q_{ij}^{\mathrm{Opt}}(E) \equiv \frac{\Phi_{ij}(E)}{n_0[I(E)/e]}, \tag{1}$$

where n_0 is the target atom number density (proportional to the gas pressure), and e is the charge of the electron.

A particular excited level i, in general, can decay to many possible lower levels. There are two ways to determine this level (or apparent as we prefer to call it) cross section in terms of the measured optical emission cross sections. The most straightforward technique is sum up the optical emission cross sections for transitions out of the level i:

$$Q_i^{\mathrm{App}}(E) = \sum_{j<i} Q_{ij}^{\mathrm{Opt}}(E). \tag{2}$$

In cases where it is difficult to measure all of the transitions out of a particular level (due to wavelengths constraints for instance), a second technique is to combine one measured optical emission cross section with experimental (or sometimes theoretical) transition probabilities:

$$Q_i^{\mathrm{App}}(E) = Q_{ij}^{\mathrm{Opt}}(E)\frac{\sum_{l<i} A_{il}}{A_{ij}}. \tag{3}$$

Note that the term in the numerator is the sum of all the transition probabilities out of the level and is equal to the inverse of the lifetime of the level. For cases where only a subset of all transitions out of a particular level can be measured, the two techniques can be combined with transition probabilities only being used to fill in the missing transitions. For example, in this paper we report measurements for the Ne($2p^5np$, $n = 4$, 5) apparent cross sections using $2p^5np \rightarrow 2p^53s$ optical emission cross section measurements combined with $2p^5np \rightarrow 2p^53s$ transition probabilities from Refs. [3,4] and lifetime measurements from Ref. [3,5,6].

There are two routes to producing an atom in a particular excited level i: direct electron-impact excitation into the level, or electron-impact excitation into higher levels that radiatively decay into the level i. The measured apparent cross sections is the sum of both the fundamental direct cross section and the cascade contribution from higher levels. In many instances, the direct cross section can be extracted from the apparent cross section by subtracting the cascade correction found by summing up all of the optical emission cross sections from higher levels that terminate on the level i. Most of the measurements reported in this paper for excitation into the higher excited levels of the rare-gases are apparent cross sections, due to the difficulties of fully measuring the cascade correction. Nonetheless, since the percentage of the cascade contribution to the signal tends to decrease for higher levels in the nonresonant series [7,8] the apparent cross section is a good approximation of the direct cross section for these levels.

3. Electronic structure and excitation cross sections

3.1. Ne($2p^5np$) configurations

The ground state of Ne is $1s^22s^22p^6\ {}^1S_0$. The first excited configuration $2p^53s$ contains four levels, called $1s_2$, $1s_3$, $1s_4$, $1s_5$ in Paschen's notation, and the next configuration $2p^53p$ contains 10 levels ($2p_1$–$2p_{10}$ in Paschen's notation). Transitions from the $2p^53p$ levels into the $2p^53s$ levels constitute the most intense part of the Ne emission spectra in the visible.

To analyze the electronic structure it is convenient to take the *LS*-coupling as a starting point and move toward the more general intermediate coupling. The $2p^53s$ configuration has four *LS*-terms, ${}^1P_1$, ${}^3P_0$, ${}^3P_1$, ${}^3P_2$. Since J is a good quantum number, the intermediate-coupling wave functions can be expresses as linear combinations of the *LS*-eigenfunctions of the same J. Thus we have two mixed levels $\alpha|{}^1P_1> + \beta|{}^3P_1>$ and $\beta|{}^1P_1> - \alpha|{}^3P_1>$, called $1s_2$ and $1s_4$, respectively, and two (unmixed) purely triplet levels ${}^3P_0$ and ${}^3P_2$ ($1s_3$ and $1s_5$). The singlet component in the $1s_2$ and $1s_4$ levels is responsible for their radiative transitions to the ${}^1S_0$ ground state. From the radiative lifetimes (1.87 ns for $1s_2$ and 31.7 ns for $1s_4$) we determine $\alpha = 0.97$ and $\beta = 0.24$. The same mixing coefficients can also be obtained from the observed g-factors. Although we seem to have a nearly *LS*-case here in that one of the $J = 1$ resonant levels is mostly singlet and the other is mostly triplet, the situation is more complicated for the other configurations as will be seen in the following paragraphs.

The 10 levels of the next configuration $2p^53p$ are formed by combining *LS*-terms of the same J out of ${}^1S_0$, ${}^3S_1$, ${}^1P_1$, ${}^3P_0$, ${}^3P_1$, ${}^3P_2$, ${}^1D_2$, ${}^3D_1$, ${}^3D_2$, and ${}^3D_3$. Here the only purely triplet level comes from the ${}^3D_3$ term which is the only level with $J = 3$ and is called the $2p_9$ level. There are two levels with $J = 0$ formed from ${}^1S_0$ and ${}^3P_0$; four levels with $J = 1$ formed out of ${}^3S_1$, ${}^1P_1$, ${}^3P_1$ and ${}^3D_1$; and three levels with $J = 2$ out of ${}^3P_2$, ${}^1D_2$, and ${}^3D_2$. For a theoretical treatment of the electronic structure, one sets up the energy matrix using the *LS*-eigenfunctions as a basis. If we represent the spin–orbit interaction by only the self-spin–orbit couplings of the 2p and 3p electrons, the energy matrix, which factors into blocks of different values of J, can be expressed in terms of Slater-Condon parameters (F's and G's) and the spin–orbit coupling constants of the 2p and 3p electrons (ζ and ζ') [9,10]. A standard procedure is to treat F_2, G_0, G_2, ζ and ζ' as adjustable parameters to fit the energy level spacing of all 10 levels. The resulting wave functions, while generally not adequate for accurate calculation of excitation cross sections, are nonetheless useful for qualitative purposes.

As a preparation for discussing how the cross sections are related to the angular momentum coupling, we start with the

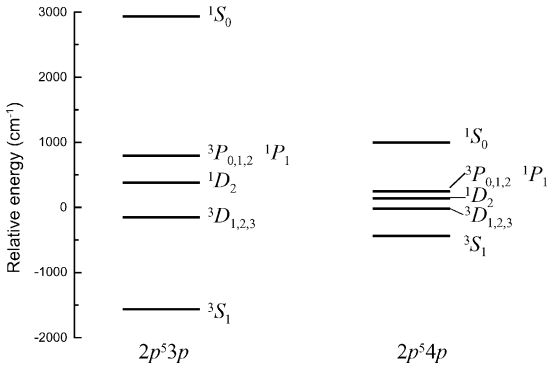

Fig. 1. Unperturbed Ne($2p^5 3p$) and Ne($2p^5 4p$) energy levels.

limit of zero spin–orbit coupling as the unperturbed system and treat the spin–orbit interaction as the perturbation. The unperturbed energies for the ^{1}S, ^{3}S, ^{1}P, ^{3}P, ^{1}D and ^{1}D terms of the $2p^5 3p$ configuration in terms of the Slater-Condon parameters given in Ref. [9] are shown in Fig. 1. The spin–orbit coupling generates matrix elements connecting *LS*-terms of the same *J*. Outside the unique case of $J = 3$, the two $J = 0$ levels are the simplest to work with since they arise from the 2×2 block of the energy matrix. Furthermore emissions from the two $J = 0$ levels are specially suited for plasma diagnostic studies [11]. Thus in this paper we focus our attention to the $J = 0$ levels to illustrate the effects of angular momentum coupling on the cross sections. In the unperturbed system the $^1S_0$ term is well above the $^3P_0$. Even with a "moderate" spin–orbit coupling, we expect a "small" mixing of these two terms and consequently a "small" upward shift for $^1S_0$ and a "small" downward shift for $^3P_0$. Of these two levels the upper one ($2p_1$) is mostly singlet and the lower one ($2p_3$) is mostly triplet. If we recall that the $1s_2$ is mostly singlet and the $1s_4$ is mostly triplet, the $2p_1 \rightarrow 1s_2$ emission must be stronger than the $2p_1 \rightarrow 1s_4$. This is reflected by optical measurements that give the branching fractions for these two channels as 0.9888 and 0.0112, respectively [12]. Likewise the $2p_3$ level decays mostly to the $1s_4$ rather than the $1s_2$, and the two branching fractions are 0.0064 and 0.9936. From the branching fractions we determine the mixing coefficients for

$$|2p_1\rangle = \xi\,|^1S_0\rangle + \eta\,|^3P_0\rangle,$$
$$|2p_3\rangle = \eta\,|^1S_0\rangle - \xi\,|^3P_0\rangle$$

as $\xi \geq 0.989$ and $\eta = 0.15$. Turning to electronic collision experiments, one notes that the cross section for excitation out of the $^1S_0$ ground state into the $2p_1$ level is the largest of the entire 2p group [13–15]. More striking is the extreme disparity in cross section between the two $J = 0$ levels ($2p_1$ and $2p_3$). For instance the $2p_1$ cross section, in units of 10^{-20} cm^2, is 185 at 50 eV, whereas the corresponding $2p_3$ cross section is 27 [14]. Likewise we see a similar disparity at 25 eV (73 and 13 for the $2p_1$ and $2p_3$ levels, respectively) and at 100 eV (137 and 22). In contrast, while their individual values are quite extreme, the average value of the two $J = 0$ level's cross sections at 50 eV (108×10^{-20} cm^2) is comparable to the average cross section (96×10^{-20} cm^2) of the three $J = 2$ levels. Since singlet-to-singlet excitation is more favorable than singlet-to-triplet excitation, the extreme disparity in the cross sections for excitation from the singlet ($2p^6$) $^1S_0$ ground state into the $2p_1$ level versus the $2p_3$ level can thus be traced back to the similar disparity in the two level's singlet composition.

The three $J = 2$ levels of $2p^5 3p$ ($2p_4$, $2p_6$, $2p_8$ in Paschen's notation) arise from $^3P_2$, $^1D_2$, and $^3D_2$. Their unperturbed energies (Fig. 1) are rather close together. Even a "small" spin–orbit interaction may result in a strong mixing of the three *LS*-terms, but there is nothing to suggest an unusual distribution of the mixing coefficients in the wave functions. In particular we expect the percentage singlet character in all three $J = 2$ levels to be of comparable magnitude. Correspondingly there is little systematic variation in the electron-impact excitation cross sections between these three levels [14]. The situation with the $J = 1$ levels is even more complicated since they are composed of four *LS* terms ($^3S_1$, $^1P_1$, $^3P_1$, $^3D_1$). With the singlet component shared fairly evenly among all four levels, the excitation cross sections into all four levels have very similar magnitudes [14].

The $2p^5 4p$ configuration of Ne ($3p_1$ through $3p_{10}$ in Paschen's notation) differs significantly from the $2p^5 3p$ configuration. In Figs. 1 and 2 we contrast the set of 3p levels with the 2p set. In the 2p manifold the top level ($2p_1$) is well above the others but the same is not true for the 3p group (see the first column in Fig. 2). In the limit of a small spin–orbit coupling the $2p_1$ level arises from the $^1S_0$ of the unperturbed system which, as seen in Fig. 1, is much higher

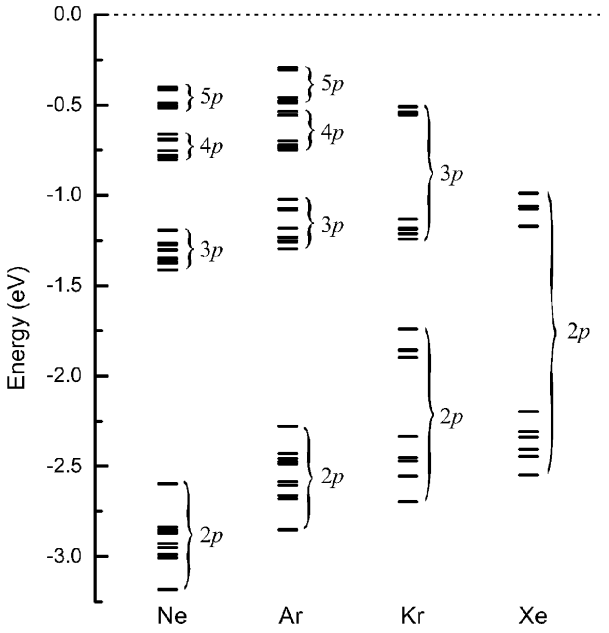

Fig. 2. Energy levels for the $n'p^5np$ configurations of Ne, Ar, Kr and Xe using Paschen's notation. The zero of the energy scale is set equal to the ionization energy.

in energy than all the other terms. For the 3p case the six unperturbed levels are compressed together by roughly a factor of three due to a reduction of the Slater-Condon factors (Fig. 1), whereas the spin–orbit coupling of the $2p^5$ core remains the same. Accordingly the top level ($3p_1$) is not as detached from the rest. The cross sections are likewise tempered, although the $3p_1$ cross sections are still significantly larger than the $3p_3$ ones (41×10^{-20} and 13×10^{-20} cm^2 at 50 eV), the disparity is not as severe as in 2p.

As we proceed to the higher configurations $2p^5np$, the energy span of the unperturbed manifold is so much reduced that it becomes less than the spin–orbit coupling parameter. The perturbative approach is no longer a convenient choice. Nevertheless we will use it to illustrate the change of the cross section pattern with the angular momentum coupling. Imagine we start with the six unperturbed terms in Fig. 1 and introduce a "large" perturbation of spin–orbit coupling. It will split the ^3P term into three components $^3P_{2,1,0}$. Since this is an inverted multiplet, the $^3P_0$ component has the highest energy. With a sufficiently large spin–orbit interaction the $^3P_0$ term is pushed above the $^1S_0$. Again the spin–orbit non-diagonal matrix elements causes $^3P_0$–$^1S_0$ mixing to form two $J = 0$ levels. Here, however, it is the upper $J = 0$ level that has a larger triplet component ($^3P_0$) and the lower $J = 0$ level that has a larger singlet component ($^1S_0$). Thus in general we expect the upper $J = 0$ level to have a smaller cross section than the lower $J = 0$ level, a reversal from the Ne($2p^5$3p) configuration where the upper $J = 0$ level ($2p_1$) has the largest cross section. This reversal is indeed observed in our measurements of electron-impact excitation cross sections. In Fig. 3 we plot our measured apparent excitation cross sections as a function of electron energy. The upper $J = 0$ level has a larger cross section than does the lower one for the $2p^5$3p and $2p^5$4p configurations ($2p_1$, $2p_3$ and $3p_1$,$3p_3$ in Paschen's notation) whereas in the case of the $2p^5$5p configuration the two $J = 0$ levels ($4p_1$ and $4p_3$) have nearly the same cross section. Curiously in Fig. 3 one finds the $3p_3$ cross sections nearly the same as the $4p_1$ and $4p_3$ cross sections. For the Ne($2p^5$6p) levels our $2p^5$6p → $2p^5$3s optical emission cross section measurements indicate that the lower $J = 0$ level has a larger cross section than does the upper one. However, we lack the needed transition probabilities to convert these into true apparent cross sections.

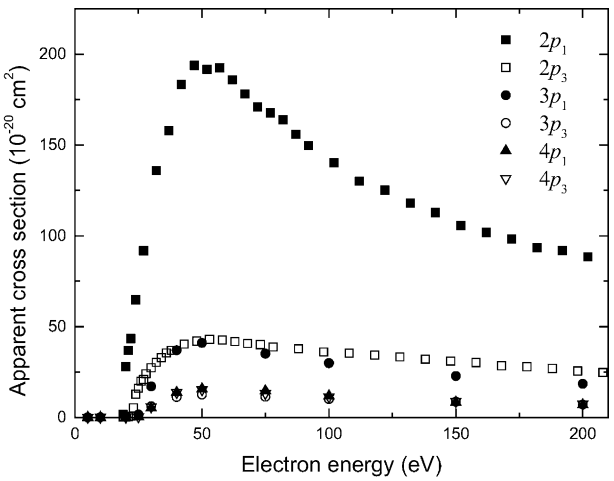

Fig. 3. Apparent electron-impact excitation cross sections as a function of electron energy for the $J = 0$ levels of the Ne($2p^5np$, $n = 3, 4, 5$) configurations. Uncertainties are ±15% for the $2p^5$3p levels and ±25% for the $2p^5$4p and $2p^5$5p levels (due to the added uncertainties from the use of transition probabilities and lifetime measurements). The $3p_3$, $4p_1$ and $4p_3$ curves are virtually indistinguishable.

In Fig. 2 we include also the energy levels of the higher Ne($2p^5np$) configurations. We notice that the energy levels change into a two-tier pattern, with an upper group of four levels and a lower group of six. This is due to a change of the angular momentum coupling. For the higher configurations the spin–orbit interaction of the $2p^5$ core remains the same but the coupling of the core with the np electron becomes smaller due to the increasing radius of the outer electron. When the 2p spin–orbit coupling significantly overpowers the other interactions, the coupling problem is somewhat simplified. Here we first deal with the $2p^5$ core alone and couple $l_c = 1$ with $s_c = 1/2$ to form the core angular momentum $j_c = 1/2$ and 3/2. The next step is to couple each j_c with both l_o and s_o to form the total angular momentum J. We refer to this as the $j_c(l_o s_o)J$ coupling as we require neither j_c to couple first with l_o to form the intermediate vector K (jK coupling) nor l_o and s_o to couple into j_o (jj coupling). To the first approximation j_c may be regarded as a good quantum number although for a more accurate description one may mix terms of the same J corresponding to different j_c.

Applying this $j_c(l_o s_o)J$ coupling scheme to a higher $2p^5np$ configuration, we combine $l_o = 1$, $s_o = 1/2$ with $j_c = 1/2$ to form $J = 0, 1, 1, 2$ (the upper four levels) and with $j_c = 3/2$ to form $J = 0, 1, 1, 2, 2, 3$ (the lower group of six). As explained before, for higher configurations the lower $J = 0$ level has a larger singlet component and thus a larger cross section than does the upper one. There is another factor that favors the cross section of the lower $J = 0$ level. The energies of the two $J = 0$ levels differ by about 0.1 eV due to the spin–orbit splitting. For the higher configurations the ionization energies of the levels are smaller, so the percentage difference in the ionization energy becomes larger. Since the ionization energy varies inversely with the atomic radius, this translates into an appreciable difference in the size of the electron cloud of the two $J = 0$ levels making the upper $J = 0$ level (with a more diffusive electron cloud) less favorable for excitation from the very compact ground state.

3.2. Ar($3p^5np$) configurations

Argon and neon are similar in their electronic structures. The two $J = 0$ levels of the Ar($3p^5$4p) configuration are again composed of the $^1S_0$ and $^3P_0$ *LS*-eigenfunctions. In

the case of Ar the two $J = 0$ levels are called $2p_1$ and $2p_5$ in Paschen's notation whereas the corresponding two levels in Ne are called $2p_1$ and $2p_3$. Again we find the upper $J = 0$ level ($2p_1$) to have a much larger cross section than the lower one ($2p_5$), e.g., 50×10^{-19} cm^2 versus 16×10^{-19} cm^2 at 20 eV [16], although the difference is not as striking as in Ne. We attribute this to a higher degree of mixing between $^1S_0$ and $^3P_0$ in the $2p_1$ and $2p_5$ wave functions of Ar because of the larger spin–orbit coupling. From the branching fractions of these two levels we determine the mixing coefficients as about 0.87/0.50 compared to 0.989/0.15 for Ne given earlier.

The same analysis of the Ne($2p^5np$) configurations also applies to the Ar($3p^5np$) configurations. The spin–orbit coupling parameter of the p^5 core is larger for Ar than Ne (954 cm^{-1} versus 521 cm^{-1}), thus the transition from the intermediate coupling in $3p^54p$ into the $j_c(l_os_o)J$ coupling for the higher n is more apparent. One manifestation of this is seen in the measurements of the excitation cross sections [17]. In Ne one has to go to the Paschen 4p levels for the two $J = 0$ levels to have comparable excitation cross sections, whereas in Ar the two $J = 0$ are nearly equal for the 3p levels, with both the $4p_5$ and $5p_5$ levels having significantly larger cross sections than the $4p_1$ and $5p_1$ levels, respectively.

3.3. Kr($4p^5np$) and Xe($5p^56p$) configurations

In going up the Ne($2p^5np$) or Ar($3p^5np$) series, as discussed in the preceding two subsections, we keep the spin–orbit coupling fixed and decrease the interaction of the core with the outer electron resulting in a gradual transition from the intermediate coupling to the $j_c(l_os_o)J$ coupling. A similar transition is made if we consider the series of Ne($2p^53p$), Ar($3p^54p$), Kr($4p^55p$) and Xe($5p^56p$). In this progression the unperturbed energy spacings are all comparable, but the spin–orbit splitting increases dramatically from 0.1 eV for Ne to 1.3 eV for Xe.

The extraordinarily large spin–orbit coupling in Xe make it a good case of $j_c(l_os_o)J$ coupling. The electron-impact excitation cross section for the lower $J = 0$ level of the Xe($5p^56p$) configuration ($2p_5$) is 10×10^{-18} cm^2 at 50 eV, which is four times larger than the cross section for excitation into the upper level ($2p_1$) [18].We also note that the $2p_5$ level has more than twice the ionization energy of the $2p_1$ level, so that the difference in electron cloud "size" (and thus the overlap with the ground state wave function) is undoubtedly an important factor in the difference in cross sections. We are unable to make a similar comparison for the $5p^57p$ configuration since the upper four levels of this configuration are above the $Xe^+(^2P_{3/2})$ limit.

The Kr($4p^55p$) configuration is an interesting intermediate case between Xe($5p^56p$) and Ar($3p^54p$). The 10 energy levels within the Kr($4p^55p$) configuration do tend towards a two-tier pattern albeit not as distinct as in Xe (see Fig. 2). The excitation cross sections for the two $J = 0$ levels also demonstrate the large role of spin–orbit coupling in creating the two-tier structure. In contrast to the lowest levels of Ne and Ar, but similar to Xe, the cross section into the lower $J = 0$ level ($2p_5$) is larger (46×10^{-19} cm^2 at 50 eV) than the upper ($2p_1$) level(24×10^{-19} cm^2) [19]. The next higher configuration Kr($4p^56p$) does show the $j_c(l_os_o)J$ coupling scheme more closely from our measurements of the optical emission cross sections for the $3p_1 \rightarrow 1s_2$ and $3p_5 \rightarrow 1s_4$ transitions. Along with transition probabilities from Ref. [3] and lifetime measurements from Refs. [20,21] we have used Eq. (3) to determine the excitation cross sections for the $J = 0$ levels of the Kr($4p^56p$) configuration. They indeed show the expected pattern of the lower $J = 0$ level ($3p_5$) having a much larger cross section, 13×10^{-19} cm^2 at 100 eV, than the upper one, 3.4×10^{-19} cm^2.

4. Conclusions

In this paper we illustrate the transition from the intermediate coupling to the $j_c(l_os_o)J$ coupling scheme in the rare-gases by looking at electron-impact excitation cross sections. Since the ground states $(n'p)^6\ ^1S_0$ for these atoms ($n' = 2$, 3, 4, 5 for Ne, Ar, Kr, Xe, respectively) conform to *LS*-coupling, we find it convenient to use the *LS*-eigenfunctions as a basis to analyze the transition from one coupling scheme to another. Two routes for this transitions were examined: (1) by decreasing the unperturbed *LS*-multiplet manifold spacing while leaving the spin–orbit splitting essentially constant, as illustrated in the Ne($2p^5np$) series with $n = 3$, 4, 5, 6; and (2) by increasing the spin–orbit splitting with only minor changes to the unperturbed *LS*-multiplet span exemplified by the Ne, Ar, Kr, Xe series. Both cases involve a gradual change of the relative weighting of the spin–orbit coupling versus the relevant Slater-Condon parameters for the *LS*-multiplets. This can be quantified by a dimensionless parameter τ defined as $\zeta/(\zeta - 15F_2 + 6G_0)$ where $6G_0 - 15F_2$ is the unperturbed $^1S_0$-$^3P_0$ spacing. This parameter ranges from $\tau = 0$ for the case of vanishing spin–orbit coupling to the other extreme of $\tau = 1$ when the interaction of the outer electron with the core is completely overwhelmed by spin–orbit effects. In Fig. 4 we show the relation between τ and the ratio of the cross section of the lower $J = 0$ level to that of the upper $J = 0$ level for the $(n'p)^5np$ configurations at 50 eV. Of special interest is that the results for all four atoms fall on the same general curve. This suggests that much of the variations in the cross section behaviors can be traced to a common ground of angular momentum coupling that is universal among the four atoms.

In recent years the studies of special characteristics of electron-impact excitation of the rare-gas atoms have been brought to the forefront in connection with applications to the optical diagnostics of low-temperature plasmas. The rare-gas emission lines are commonly used as a diagnostic tool for rare-gas plasmas or other plasmas containing rare-gas atoms as a tracer [22–25]. In weakly-ionized

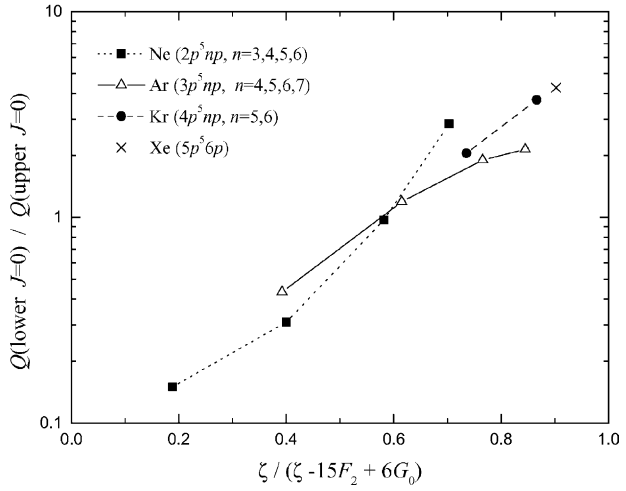

Fig. 4. Comparison of the cross section ratio of the two $J = 0$ levels for the $n'p^5np$ configurations. The limit of the abscissa going to zero corresponds to *LS* coupling, while a value of 1 corresponds to *jj* coupling.

plasmas where excited atoms are primarily excited by electron-atom collisions, the intensity of the $x \rightarrow y$ emission line can be used to monitor the plasma electron energy distribution in the energy region from the threshold of level-x on up, provided the $x \rightarrow y$ optical emission cross section is known. By considering a number of levels with different excitation threshold energies, the electron temperature can be determined. However, excited levels can also be populated by excitation out of metastable levels with a much lower threshold energy (i.e., 1.5 eV versus 13 eV for Ar). Recent experiments [26,27] have shown, however, that the excitation cross sections of metastable atoms into the $(n'p)^5np$ $J = 0$ levels are very small, indicating that these levels in a plasma are populated almost entirely by excitation out of the ground level. The $J = 0$ $(n'p)^5np$ levels examined in this paper cover a wide range of excitation threshold energies (9–21 eV), permitting measurements of the plasma emission lines from these levels in combination with excitation cross sections to provide detailed information about the electron energy distribution function.

Acknowledgements

This work was supported by the Air Force Office of Scientific Research.

References

[1] W.L. Nighan, IEEE Trans. Electron Devices 28 (1981) 625.
[2] A.R. Filippelli, C.C. Lin, L.W. Anderson, J.W. McConkey, Adv. At. Mol. Opt. Phys. 33 (1994) 1.
[3] NIST Atomic Spectra Database, URL: http://physics.nist.gov/asd.
[4] M.J. Seaton, J. Phys. B 31 (1998) 5315.
[5] J.E. Hesser, Phys. Rev. 174 (1968) 68.
[6] P. Martin, J. Campos, J. Phys. B 10 (1977) 1265.
[7] J.O. Phelps, J.E. Solomon, D.F. Korff, C.C. Lin, E.T.P. Lee, Phys. Rev. A 20 (1979) 1418.
[8] J.O. Phelps, C.C. Lin, Phys. Rev. A 24 (1981) 1299.
[9] E.U. Condon, G.H. Shortley, The Theory of Atomic Spectra, Cambridge University Press, London, 1963.
[10] R.D. Cowan, K.L. Andrew, J. Opt. Soc. Am. 55 (1965) 502.
[11] C.C. Lin, Contributions to Plasma Physics, 2004, in press.
[12] J.E. Chilton, Ph.D. Thesis, University of Wisconsin, 1999.
[13] F.A. Sharpton, R.M. St John, C.C. Lin, F.E. Fajen, Phys. Rev. A 2 (1970) 1305.
[14] J.E. Chilton, M.D. Stewart Jr., C.C. Lin, Phys. Rev. A 61 (2000) 052708.
[15] S. Tsurubuchi, K. Arakawa, S. Kinokuni, K. Motohashi, J. Phys. B 33 (2000) 3713.
[16] J.E. Chilton, J.B. Boffard, R.S. Schappe, C.C. Lin, Phys. Rev. A 57 (1998) 267.
[17] T. Weber, J.B. Boffard, C.C. Lin, Phys. Rev. A 68 (2003) 032719.
[18] J.T. Fons, C.C. Lin, Phys. Rev. A 58 (1998) 4603.
[19] J.E. Chilton, M.D. Stewart Jr., C.C. Lin, Phys. Rev. A 62 (2000) 032714.
[20] A. Delgado, J. Campos, C. Sanchez del Rio, Z. Phys. 257 (1972) 9.
[21] M.V. Fonseca, J. Campos, Phys. Rev. A 17 (1978) 1080.
[22] D.J. Smith, C.J. Whitehead, R. Stewart, Plasma Sour. Sci. Technol. 11 (2002) 115.
[23] G. Franz, A. Kelp, P. Messerer, J. Vac. Sci. Technol. A 18 (2000) 2053.
[24] M.V. Malyshev, V.M. Donnelly, J. Vac. Sci. Technol. A 15 (1997) 550.
[25] M.V. Malyshev, V.M. Donnelly, Phys. Rev. E 60 (1999) 6016.
[26] G.A. Piech, J.B. Boffard, M.F. Gehrke, L.W. Anderson, C.C. Lin, Phys. Rev. Lett. 81 (1998) 309.
[27] J.B. Boffard, M.L. Keeler, G.A. Piech, L.W. Anderson, C.C. Lin, Phys. Rev. A 64 (2001) 032708.